Advances in Physics Theories and Applications
ISSN 2224-719X (Paper) ISSN 2225-0638 (Online)
Vol.65, 2017

Study the Lattice Distortion and Particle Size of One Phase of MnO by Using Fourier Analysis of X-ray Diffraction Lines

Khalid Hellal Harbbi Sarab Saadi Jahil
Department of Physics – College of Education (Ibn Al-Haitham) – University of Baghdad, Iraq

Abstract
In this study, the Fourier analysis method was used for the analysis of the X-ray diffraction pattern of MnO (111), (200), (220), (311) and (222). The particle size of each X-ray line was calculated, the particle size of the manganese oxide was then calculated. The Fourier method was also used to calculate the mean square lattice strain of the manganese oxide and the results were as follows, where the particle size is equal to 7.9563 nm and the mean square strain equal to 0.3566×10^{-4}. In order to determine the accuracy of the results of this method, other methods of analysis were used, such as the Debye - Scherrer method and Williamson–Hall method of analysis, and Modified Scherrer equation for calculating the particle size. The value of particle size and strain of these four methods was compared with the value of particle size and mean square strain of the Fourier method.
Keywords: Lattice Distortion, Particle Size, Fourier analysis, X-ray Diffraction Lines

1. Introduction

Diffraction peak profile analysis (or Line Profile Analysis, LPA) has recently been developed to such an extent that it can be applied as a powerful method for the characterization of microstructures of crystalline materials in terms of crystallite size-distribution and dislocation structures. Physically based theoretical functions and their Fourier coefficients are available for both, the size and the strain diffraction profiles. Strain anisotropy is rationalized in terms of the contrast factors of dislocations [Ungar & Gubicza]. X-ray diffraction profiles using Fourier analysis for single crystal Al and Cu samples subjected to micro scale laser shock penning. Specifically, the asymmetric and broadened diffraction profiles registered across the shock peen region were analyzed by the Fourier analysis method. Average strain, particle size and dislocation density[Chen & Yao 2004]. There are two basic techniques of x-ray line profile analysis: (i) Fourier space technique under which Fourier analysis (Warren 1968) also forms a part, and (ii) real space techniques like (a) integral breadth (Wagner and Aqua 1964), (b) variance analysis (Wilson 1962) and (c) peak- fitting methods (Keijser*et al* 1982). It has been shown that each of the above techniques leads to similar results for domain size, dislocation density etc [KAPOOR& LAHIRI 2004].The well-known Scherrer equation explains peak broadening in terms of incident beam divergence which makes it possible to satisfy the Bragg condition for non-adjacent diffraction planes. Once instrument effects have been excluded, the crystallite size is easily calculated as a function of peak width (specified as the full width at half maximum peak intensity (FWHM)), peak position and wavelength. Warren and Averbach's method takes not only the peak width into account but also the shape of the peak. This method is based on a Fourier deconvolution of the measured peaks and the instrument broadening to obtain the of true diffraction profile. This method is capable yielding both the crystallite size distribution and lattice micro strain[RIELLA, MARTINEZ&. IMAKUMA1988].In the case of sampled diffraction patterns, as in crystallography, Fourier refinement methods generally require a good approximation to the real solution before refinement is at all meaningful. The continuity of the observed Fourier transform partially removes this condition. One further piece of information, namely knowledge that the structure is of finite rather than infinite thickness, is sufficient to restrict the number of possible solutions to a very small number, and often to just one[ROBERT & DAVID 1979]. In this study was selected the particle size and mean square strain of x- ray diffraction pattern of MnO nanoparticles using Cu Kα as shown in figure (1) [Berman &Cohen 1990].

2. Theory

2.1 The Fourier Analysis Method

x-ray diffraction pattern of a crystal can be described in terms of cattering intensity as function of scattering direction defined by the scattering angle 2θ , or by the scattering parameters = $2 \sin\theta/ \lambda$, where λ is wavelength of the incident radiation. Experimentally one can measure the integrated intensity profile function $h(2\theta)$ or h(s) for the crystals. We shall discuss the X-ray diffraction for the mosaic structure model in which the atoms are arranged in blocks, each block itself being an ideal crystal, but with adjacent blocks not accurately fitted together. The experimental X-ray line profile (XRLP), (h) it is represents the convolution between the true sample (f) and the instrumental function produced by a well-annealed sample and (g) it is described by the integral equation of the first kind [Karen& Woodward 1998].In addition to the line broadening due to the particle size and strain ,there is a source of broadening due to the equipment itself (slit size , penetration in the sample ,imperfect focusing).The source of broadening is called "instrumental broadening" . A correction for the contribution of the instrumental broadening can be made considering that the x erimental profile h(x) is a convolution of the sample

profile f(x) and the nstrumental contribution g(x).

h(x) = f(x) × g(x……(1)

Using the properties of Fourier series ,Stokes [Warren 1969]. Demonstrated that f(x)could be obtained from the Fourier coefficient of g(x) and h(x).The g(x) profile is obtained through the standard sample ,in the same conditions as the experimental profile h(x) [Stokes 1948]. Determination of the pure specimen-broadened profile as mentioned before the specimen's size and strain broadening can be obtained, the observed profile must be corrected for instrumental broadening. Most used methods are the Fourier-transform deconvolution method [Vives& Gaffet 2004,Smith 1934] and simplified integral-breadth methods that rely on some assumed analytical forms of the peak profiles. The iterative method of successive folding [Stokes 1948,Burger 1932] is not used extensively, and will not be considered here. Deconvolution method of Stokes from equation (1), it follow that deconvolution can be performed easily in terms of Fourier transforms of respective functions:

H(L) = G(L)F……(2)

where F(L), H(L) and G(L) are Fourier transforms of the true sample, experimental and instrumental function, respectively. The variable L is the distance perpendicular to the (hkl) reflection planes . The crystallite size and lattice disorder can be analyzed as a set of the independent events of likelihood concept. The normalized F(L) can be described as the product of two factors, $F_{(L)}^{s} and\ F_{(L)}^{\varepsilon}$The factor $F_{(L)}^{s}$describes the contribution of crystallite size and stocking fault probability while the factor $F_{(L)}^{\varepsilon}$ gives information about the mean square strain of the lattice. Based on Warren and Averbach theory [Ergun 1968], the general form of the Fourier transform of the true sample for cubic lattices is given by relationships :

$$F^{(s)}(L) = e^{-\frac{|L|}{Deff_{(hkl)}}} \quad \text{……(3)}$$

$$F^{(\varepsilon)}(L) = e^{-\frac{2\pi^2<\varepsilon_L^2>h_s^2 L^2}{a^2}} \quad \text{…… (4)}$$

Where $D_{(hkl)}^{eff}$ is the effective size $< \varepsilon^2 >_{hkl}$ Is the micro strain of the lattice , $h_s^2 = h^2+k^2+l^2$ and $c^2 = 2\pi^2 h_s^2/a^2$ it is known that whenever two or more x-ray line profiles (XRLP)of the same (hkl) plane family are present the particle size and the lattice disorder effects can be separated [Klug& Alexander 1974].

Diffraction from crystal planes occurs at welled fined angles that satisfy the Bragg equation

nλ = 2d sinθ …… (5)

Theoretically, intensity diffracted from an infinite crystal should consist of diffraction lines without width (Dirac delta functions) at some discrete diffraction angles. However, both instrument and specimen broaden the diffraction lines, and the observed line profile is a convolution of three functions[Raiteri &Senin 1978,Taupin 1973]. L is the Fourier length, defined as $L = na3$, where n is the integer and $a3$ the unit of the Fourier length in the direction of the diffraction :

$a3 = \lambda /2(\sin \theta 2 - \sin \theta 1)$ …… (6)

where the line profile is measured from $\theta 1$ to $\theta 2$ and λ is the wavelength of the x-rays .

2.2 Debye - Scherrer Method

The Debye - Scherrer equation, is a formula that relates the size of sub-micro metre particles, or crystallites, in a solid to the broadening of a peak in a diffraction pattern [Huang& Parrish , Patterson 1939]. It is used in the determination of size of particles of crystals in the form of powder. The Scherrer equation can be written as:

D = Kλ /β cosθ…… (7)

where D is the mean size of the ordered (crystalline) domains, which maybe smaller or equal to the grain size K is a dimensionless shape factor, and the value is taken to be 0.9 ; λ is the x-ray wavelength; β is the line broadening at half the maximum intensity (FWHM), This quantity is also sometimes denoted as Δ (2θ); θ is the Bragg angle measured. From the results it is concluded that the crystallite size is less than 100 nm .Scherrer equation D =$\frac{k\,\lambda}{\beta\ cos\theta}$ was developed to calculate the nano crystallite size (D) by XRD radiation of wavelength λ (nm) from measuring full width at half maximum of peaks (β) in radian located at any 2θin the pattern. Shape factor of K can be 0.62 - 2.08 and is usually taken as about 0.89. But, if all of the peaks of a pattern are going to give a similar value of D, then β .cosθ must be identical.The purpose of modified Scherrer equation given in this paper is to provide a new approach to the kind of using Scherrer equation, so that a least squares technique can be applied to minimize the sources of errors. Modified Scherrer equation plots ln βagainst ln(1/cosθ) and obtains the intercept of a least squares line regression, ln kλ/L, from which a single value of L is obtained through all of the available peaks [Scherrer 1918]. This method seems valid as it gives intermediate values between Lorentzian and Gaussian assumptions then we can write the Scherrer equation as:

$$\beta_{\Delta 2\theta(hkl)} = \frac{k\times\lambda}{L_{hkl}\times cos\theta_D} \quad \text{……(8)}$$

where λ the wavelength, 2θ is the Bragg angle of reflection, and β

is the integral breadth in radian [Anitha & Jayakumar 2015,Eric 2008]. And also calculate the strain from the equation :

$\beta = 4\varepsilon \tan\theta$ ……(9)

2.3 Williamson–Hall method

The strain induced in powders due to crystal imperfection and distortion was calculated using the formula:

$\varepsilon = \frac{\beta_{(hkl)}}{4\tan\theta}$ …… (10)

the crystallites size D is less than 1 μ m exhibit profile broadening. The integral breadth in radians is due to the effect of small crystallites is related to D by the equation [Delhez 1982],

$D = \frac{K\lambda}{\beta_{hkl}\cos\theta}$ ……(11)

width from crystallite size varies as $\frac{1}{\cos\theta}$, strain varies as $\tan\theta$ as suming that the particle size and strain contributions to line broadening are independent to each other . The observed line breadth is simply the sum of equations (10) and (11) as:

$\beta_{hkl} = K\lambda/D\cos\theta + 4\varepsilon\tan\theta$ …… (12)

[24,Stokes 1944] . Multiplying both sides of equation (12) by cos θ, we obtain :

$\beta_{hkl}\cos\theta = \frac{k\lambda}{D} + 4\varepsilon\sin\theta$ ……(13)

is regarded as a straight line, y = ax + b. A plot of y = β cosθ against x = sinθ is referred to as the Williamson–Hall (WH) plot since Williamson and Hall [Balzar 2004] proposed this methodology. However, this designation is somewhat unfair because Hall was the first to report the idea [Williamson &Hall 1953]. The slope of the straight line is ε while its y intercept is kλ/D. Equation (13) holds true for isotropic line broadening. If both of crystallite-size and micro strain profiles are Gaussian, then the plot is convex downward, having the same terminal slope at a high angle as the Lorentzian case and intercepting the y axis at kλ/D [Hall 1949]. The W-H plot is a very useful diagnostic tool for learning the kinds of profile broadening and determining approximate values of D and ε [Kisi& Howard].

2.4 Modified Scherrer Method

It is assumed that if there are N different peaks of a specific nanocrystal , then all of these N peaks must present identical *L* values for the crystal size. But, during the extensive research of the first author of thins paper, on different nano ceramic crystals, which were synthesized or mi-nerally achieved, it was surprisingly observed that each peak yields a different value and there is a systematic error on the results obtained from each peak .Further investigation approved the presence of a systematic error in Scherrer formula. In fact since

$D = \frac{K\lambda}{\beta.\cos\theta}$ ……(14)

If D is going to be a fixed value for different peaks of a substance, considering that k and λ and therefore kλ are fixed values, then it is essential that β.cos θ be a fixed multiple during .This has never been observed and cannot be true. Modified Scherrer formula is based on the face that we must decrease the errors and obtain the average value of D though all the peaks (or any number of selected peaks) by using least squares method to mathematically de-crease the source of errors.

We can write the basic Scherrer formula as:

$\beta = \frac{K\lambda}{D} \cdot \frac{1}{\cos\theta}$ …… (15)

$\ln\beta = \ln\frac{K\lambda}{D} + \ln\frac{1}{\cos\theta}$ ……(16)

If we plot the results of ln β against ln (1 / cosθ) we get a straight line on the curve with an intercept of Y- axis and the particle size must be obtained from the point of this intercept which is most accurate . After getting the intercept, then the exponential of the intercept is obtained [Lzumi 2014]:

$e^{\ln\frac{k\lambda}{D}} = e^{intercept} = \frac{K\lambda}{D}$ …… (17)

3. Results and Discussion

3.1 Fourier analysis method

The Fourier method was used to analyze x - ray diffraction lines for MnO nanoparticles whereas contains five lines, such as (111) , (200) , (220) , (311) and (222) respectively (for manganese mono oxide JCPDF Card number 07-0230) with cubic system and face centered cubic lattice. The strong peaks along the plane (2 0 0), (1 1 1), and (2 2 0) indicate that the obtained product is highly crystalline and has grown in these directions. The figure (2) shows the values of h(x) of line profile (111) which is represent the values of the intensity for each of the twenty steps, ten of which are on the right and the other ten on the left . The beginning and end of the steps were determined by the beginning and end of the X-ray diffraction line tails. After h(x) values were collected

from right and their values from the left. The average values of Hr (t) were calculated for different values of variable (t) such as t = 0,1,2,3,4,5,6,7,8,9 and 10 and the result listed in the Table (1). The values of g(x) of line profile which is represent the values of the intensity for each of the twenty steps, ten of which are on the right and the other ten on the left for the line of diffraction that returns to the standard model and usually uses quartz as a single crystal. The ten values of g(x) . Each value was obtained for one value of (t) , and g(x) values were obtained for Gr(t) and the results are listed in Table (2) . Equation (2) was used to calculate the value Fr (t) for each value of H r(t) and Gr(t) , and the results were included in the Table (3). The same calculations were made for other x-ray diffraction lines such as (200), (220) , (311) and (222) and the results of Fr (t) , Hr(t) and Gr(t) are listed in Tables (4) ,(5) ,(6) and (7) respectively . The rate (Fr) t was then taken for each line of diffraction lines (111) , (200) , (220) , (311) and (222) Then the equations (3) and (4) were used to determine the particle size D and lattice strain $< \varepsilon^2 >$ respectively for the lines (111) , (200) . (220) , (311) and (222) and the results are set out in the Table (8) and this Table shows that the crystallite size increase with decrease the lattice strain this result is fails in some times because extract information regarding the size distribution and strain profile by analyzing the theta dependence of the cosine Fourier coefficients (which describe the symmetric broadening) . Therefore the disproportion between particle size and strain due to the some liens are not symmetric broadening .

3.2 Debye - Scherrer Method

In this method, equation (7) is used to calculate the particle size of each line of diffraction lines and β in equation (7) represents FWHM calculated in radians and the wavelength of the copper is used equal to 0.15046 nm and listed the result in Table (9) . also this Table shows the values of strain which was calculated using the equation (8) . In this method we can see that the inverse the relation between the particle size and strain .

3.3 Williamson–Hall Method

In this study we have analyzed line diffraction profile by Williamson –Hall method ,we have used Figure (3)to calculate FWHM (β_{hkl}) and Then we have used FWHM (β_{hkl}) and 2θ to determine the $\beta_{hkl}\cos\theta$ and $4\sin\theta$ for each peak MnO nano particles ,the results are listed in Table (10) ,the expression $\beta_{hkl}\cos\theta$ is the y-axis and $4\sin\theta$ is the x-axis in Williamson –hall plot as shown in Figure (3). Williamson –hall plot have been used to calculate the crystallite size D and the lattice strain ε by using equation (13) .Graphically, the crystallite size D is obtained from the y-intercept and the lattice strain ε obtained from the slope . From the Figure (3) we get :

$D = \frac{k\lambda}{intercept}$

D = 9.864 nm

As well from the slope represent values ε strain , then

$\varepsilon = 20.833 * 10^{-4}$

This method gives the results more accurate from Debye - Scherrer method because used the straight line which is gives the particle size (from the y-intercept) and the strain (from the slope) in one times .

3.4 Modified Scherrer Method

In this method equation (16) was used and plot the results of ln β against ln(1 / cosθ) for the lines (111) , (200) ,(220) , (311) and (222) to get a straight line as shown in the Figure (4) . And from intercept of Y- axis we can get on the particle size because the intercept equal to ln (k λ/D) . After getting the intercept, then the value of the intercept is

Obtained by the equation:

$D = e^{k\lambda/cutting}$

Where k =0.9 and λ_{cu} = 0.15405 nm , then

D = 6.5081 nm

In this method used the diagram to calculate the average particle size for all lines (111) , (200) , (220) , (311) and (222) as shown in Table (11) ,therefore the value of particle size is different something from the value which is obtained by Scherrer method insipid of the two methods used full width at half maximum height, FWHM or β .Thus we can see the final results in Fourier analysis method and the other methods of analysis used in this work in Table (12) . The difference in the results of the calculation of crystallite size and strain between the Fourier method and other methods of analysis is the high accuracy in calculating the intensity of the diffraction curve in the Fourier method where this method is based on the calculation of the area under the curve.

4. Conclusions

1. Crystallize sizes below roughly 100 nm can accurately be evaluated using powder diffraction techniques.
2.Microstrain, which arises due to point defects (vacancies, site disorder), dislocations and even extended defects can be evaluated using powder diffraction techniques.

3.The Debye Sherrer method does not give accuracy in the results because of the adoption of this method at the highest intensity without taking into account the intensity of integrated. This means that FWHM take only part of the X-ray diffraction line area.
4. The Debye -Sherrer equation can be developed in the computation of emotion as a new model The Debye - Sherrer equation can be developed in the computation of strain as a new model for the purpose of comparing results with other methods of analysis. Because Sherrer gives a volume connector. In general, this method gives results different from the way Debye - Sherrer because it is used in calculating the average particle size and strain through the plot .
5. In the Williamson -Hull method, particle size and strain are calculated by the constructor diagram that links the two variables. Therefore, the results of this method differ from the results of the Modified - Sherrer method , although both methods depend on FWHE calculations
6. When comparing the Fourier method in the analysis of x-ray diffraction lines and the methods of analysis used in this work. It was concluded that the results of the Fourier method are the most accurate results because this method is based mainly on the analysis of the X-ray diffraction line, starting from the line tails up to the top for the intensity and diffraction angle. Fourier methods are the most general method for extracting volume and intensity but require high accuracy in diffraction line analysis as well as in calculating granular size and emotion separately from each other.

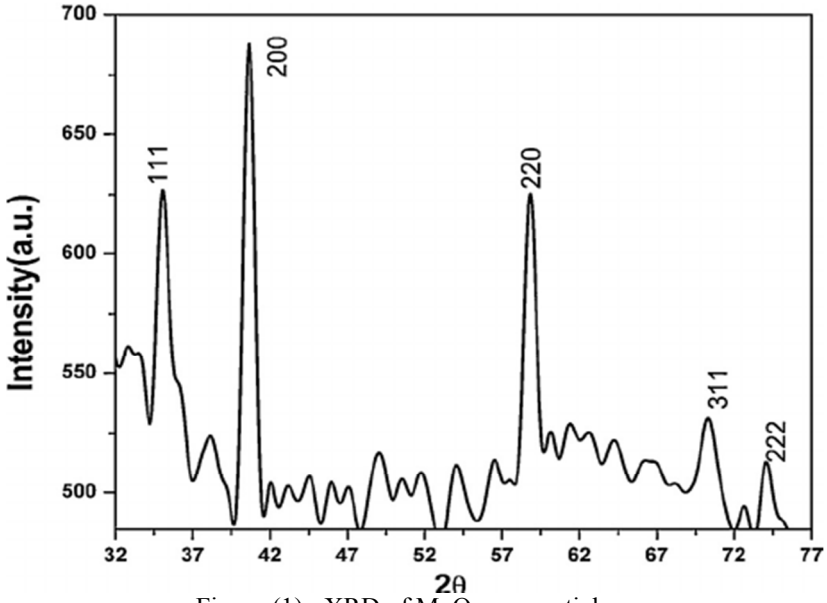

Figure (1) : XRD of MnO nanoparticles .

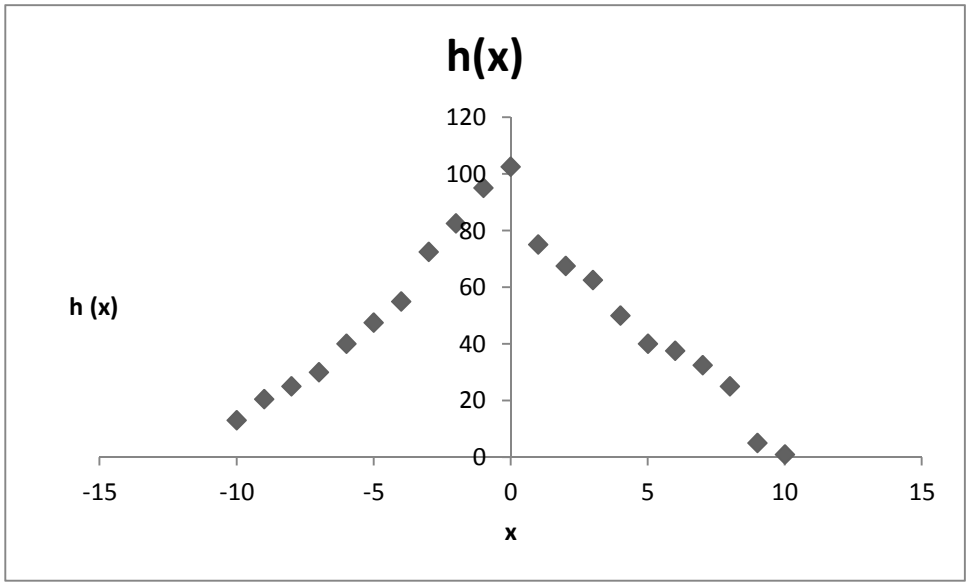

Figure (2) : h(x) against x of the line (111) .

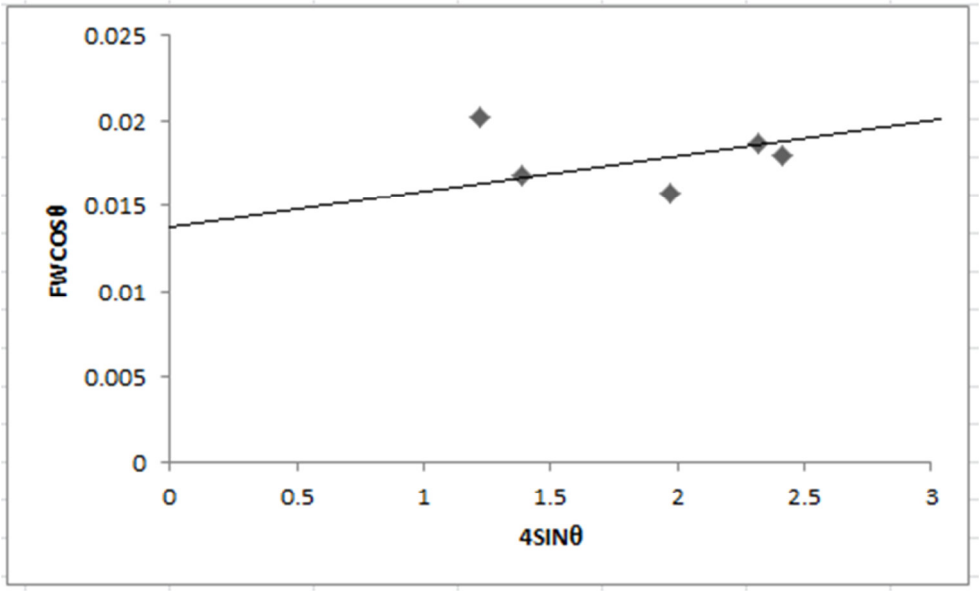

Figure (3): Williamson –hall plot of β_{hkl} cosθ ,4sinθ of MnO nanoparticles.

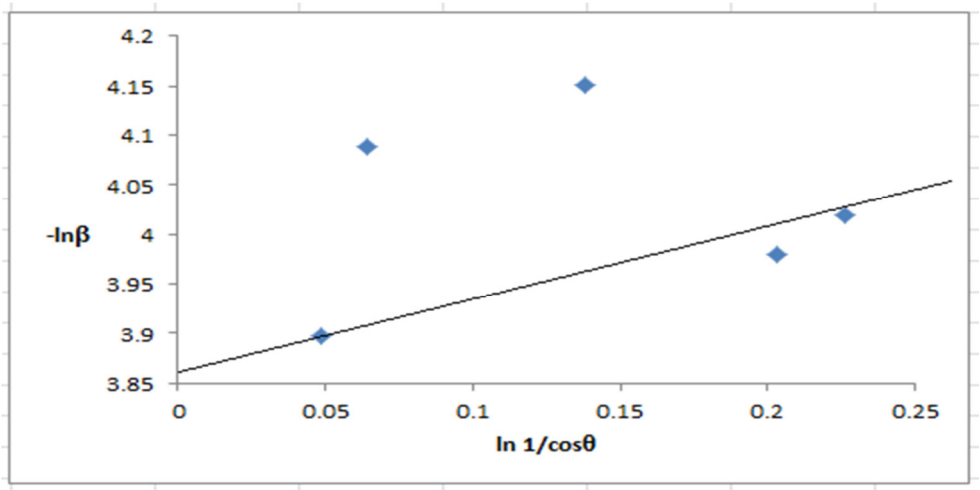

Figure (4) : The relation between ln 1/cosθ on the y-axis and ln β on the x- axis of modified Scherrer method.

Table (1) : the values of h(x) for (111) peak and (x) and Hr(t) at all values of t from 0 to 10, at (t = 0)

x	h(x)	(2πxt)/60	cos(2πxt)/60	h(x)cos(2πxt)/60	x	h(x)	(2πxt)/60	cos(2πxt)/60	h(x)cos(2πxt)/6	Hr(t)
0	103	0	1	102.5						97.95
1	75	0	1	75	-1	95	0	1	95	
2	68	0	1	67.5	-2	83	0	1	82.5	
3	63	0	1	62.5	-3	73	0	1	72.5	
4	50	0	1	50	-4	55	0	1	55	
5	40	0	1	40	-5	48	0	1	47.5	
6	38	0	1	37.5	-6	40	0	1	40	
7	33	0	1	32.5	-7	30	0	1	30	
8	25	0	1	25	-8	25	0	1	25	
9	5	0	1	5	-9	21	0	1	20.5	
10	1	0	1	1	-10	13	0	1	13	
				498.5					481	

at(t = 1)

x	h(x)	(2πxt)/60	cos(2πxt)/60	h(x)cos(2πxt)/60	x	h(x)	(2πxt)/60	cos(2πxt)/60	h(x)cos(2πxt)/6	Hr(t)
0	103	0	1	102.5						88.307
1	75	0.10467	0.9945274	74.58955824	-1	95	-0.1047	0.9945274	94.48010711	
2	68	0.20933	0.9781697	66.02645277	-2	83	-0.2093	0.9781697	80.69899783	
3	63	0.314	0.9511057	59.4441075	-3	73	-0.314	0.9511057	68.9551647	
4	50	0.41867	0.9136318	45.68159046	-4	55	-0.4187	0.9136318	50.2497495	
5	40	0.52333	0.8661581	34.64632378	-5	48	-0.5233	0.8661581	41.14250948	
6	38	0.628	0.8092042	30.34515679	-6	40	-0.628	0.8092042	32.36816724	
7	33	0.73267	0.7433934	24.16028667	-7	30	-0.7327	0.7433934	22.30180308	
8	25	0.83733	0.6694462	16.73615413	-8	25	-0.8373	0.6694462	16.73615413	
9	5	0.942	0.5881717	2.940858652	-9	21	-0.942	0.5881717	12.05752047	
10	1	1.04667	0.5004597	0.500459689	-10	13	-1.0467	0.5004597	6.505975957	
				457.5709487					425.4961495	

at (t = 2)

x	h(x)	(2πxt)/60	cos(2πxt)/60	h(x)cos(2πxt)/60	x	h(x)	(2πxt)/60	cos(2πxt)/60	h(x)cos(2πxt)/6	Hr(t)
0	103	0	1	102.5						63.971
1	75	0.20933	0.9781697	73.3627253	-1	95	-0.2093	0.9781697	92.92611871	
2	68	0.41867	0.9136318	61.67014712	-2	83	-0.4187	0.9136318	75.37462425	
3	63	0.628	0.8092042	50.57526131	-3	73	-0.628	0.8092042	58.66730312	
4	50	0.83733	0.6694462	33.47230826	-4	55	-0.8373	0.6694462	36.81953909	
5	40	1.04667	0.5004597	20.01838756	-5	48	-1.0467	0.5004597	23.77183523	
6	38	1.256	0.3096228	11.61085549	-6	40	-1.256	0.3096228	12.38491252	
7	33	1.46533	0.1052676	3.421197037	-7	30	-1.4653	0.1052676	3.158028034	
8	25	1.67467	-0.1036837	-2.59209159	-8	25	-1.6747	-0.103684	-2.59209159	
9	5	1.884	-0.308108	-1.540540156	-9	21	-1.884	-0.308108	-6.316214641	
10	1	2.09333	-0.4990802	-0.499080199	-10	13	-2.0933	-0.49908	-6.488042592	
				351.9991701					287.7060121	

at (t = 3)

x	h(x)	(2πxt)/60	cos(2πxt)/60	h(x)cos(2πxt)/60	x	h(x)	(2πxt)/60	cos(2πxt)/60	h(x)cos(2πxt)/6	Hr(t)
0	103	0	1	102.5						35.834
1	75	0.314	0.9511057	71.332929	-1	95	-0.314	0.9511057	90.35504339	
2	68	0.628	0.8092042	54.62128222	-2	83	-0.628	0.8092042	66.75934493	
3	63	0.942	0.5881717	36.76073315	-3	73	-0.942	0.5881717	42.64245045	
4	50	1.256	0.3096228	15.48114065	-4	55	-1.256	0.3096228	17.02925472	
5	40	1.57	0.0007963	0.031853068	-5	48	-1.57	0.0007963	0.037825519	
6	38	1.884	-0.308108	-11.55405117	-6	40	-1.884	-0.308108	-12.32432125	
7	33	2.198	-0.5868829	-19.07369583	-7	30	-2.198	-0.586883	-17.60648846	
8	25	2.512	-0.8082674	-20.20668568	-8	25	-2.512	-0.808267	-20.20668568	
9	5	2.826	-0.9506126	-4.753062991	-9	21	-2.826	-0.950613	-19.48755826	
10	1	3.14	-0.9999987	-0.999998732	-10	13	-3.14	-0.999999	-12.99998351	
				224.1404437					134.1988818	

at (t = 4)

x	h(x)	(2πxt)/60	cos(2πxt)/60	h(x)cos(2πxt)/60	x	h(x)	(2πxt)/60	cos(2πxt)/60	h(x)cos(2πxt)/6	Hr(t)
0	103	0	1	102.5						14.511
1	75	0.41867	0.9136318	68.52238568	-1	95	-0.4187	0.9136318	86.79502187	
2	68	0.83733	0.6694462	45.18761616	-2	83	-0.8373	0.6694462	55.22930864	
3	63	1.256	0.3096228	19.35142582	-3	73	-1.256	0.3096228	22.44765395	
4	50	1.67467	-0.1036837	-5.18418318	-4	55	-1.6747	-0.103684	-5.702601498	
5	40	2.09333	-0.4990802	-19.96320797	-5	48	-2.0933	-0.49908	-23.70630947	
6	38	2.512	-0.8082674	-30.31002852	-6	40	-2.512	-0.808267	-32.33069709	
7	33	2.93067	-0.9778375	-31.77971759	-7	30	-2.9307	-0.977837	-29.33512393	
8	25	3.34933	-0.9784994	-24.4624849	-8	25	-3.3493	-0.978499	-24.4624849	
9	5	3.768	-0.8101389	-4.050694411	-9	21	-3.768	-0.810139	-16.60784708	
10	1	4.18667	-0.5018379	-0.501837909	-10	13	-4.1867	-0.501838	-6.52389282	
				119.3092732					25.80302766	

at(t = 5)

x	h(x)	(2πxt)/60	cos(2πxt)/60	h(x)cos(2πxt)/60	x	h(x)	(2πxt)/60	cos(2πxt)/60	h(x)cos(2πxt)/6	Hr(t)
0	103	0	1	102.5						4.6931
1	75	0.52333	0.8661581	64.96185708	-1	95	-0.5233	0.8661581	82.28501897	
2	68	1.04667	0.5004597	33.78102901	-2	83	-1.0467	0.5004597	41.28792434	
3	63	1.57	0.0007963	0.049770419	-3	73	-1.57	0.0007963	0.057733687	
4	50	2.09333	-0.4990802	-24.95400997	-4	55	-2.0933	-0.49908	-27.44941096	
5	40	2.61667	-0.865361	-34.61444142	-5	48	-2.6167	-0.865361	-41.10464919	
6	38	3.14	-0.9999987	-37.49995244	-6	40	-3.14	-0.999999	-39.99994927	
7	33	3.66333	-0.866953	-28.17597108	-7	30	-3.6633	-0.866953	-26.00858869	
8	25	4.18667	-0.5018379	-12.54594773	-8	25	-4.1867	-0.501838	-12.54594773	
9	5	4.71	-0.002389	-0.011944891	-9	21	-4.71	-0.002389	-0.048974051	
10	1	5.23333	0.4976994	0.497699444	-10	13	-5.2333	0.4976994	6.470092769	
				63.98808842					-17.05675012	

at (t = 6)

x	h(x)	(2πxt)/60	cos(2πxt)/60	h(x)cos(2πxt)/60	x	h(x)	(2πxt)/60	cos(2πxt)/60	h(x)cos(2πxt)/6	Hr(t)
0	103	0	1	102.5						4.023
1	75	0.628	0.8092042	60.69031357	-1	95	-0.628	0.8092042	76.87439719	
2	68	1.256	0.3096228	20.89953988	-2	83	-1.256	0.3096228	25.54388208	
3	63	1.884	-0.308108	-19.25675195	-3	73	-1.884	-0.308108	-22.33783227	
4	50	2.512	-0.8082674	-40.41337136	-4	55	-2.512	-0.808267	-44.4547085	
5	40	3.14	-0.9999987	-39.99994927	-5	48	-3.14	-0.999999	-47.49993976	
6	38	3.768	-0.8101389	-30.38020808	-6	40	-3.768	-0.810139	-32.40555528	
7	33	4.396	-0.3111368	-10.11194631	-7	30	-4.396	-0.311137	-9.334104284	
8	25	5.024	0.3065925	7.664811699	-8	25	-5.024	0.3065925	7.664811699	
9	5	5.652	0.8073286	4.036643117	-9	21	-5.652	0.8073286	16.55023678	
10	1	6.28	0.9999949	0.999994927	-10	13	-6.28	0.9999949	12.99993405	
				56.62907622					-16.39887829	

at (t = 7)

x	h(x)	(2πxt)/60	cos(2πxt)/60	h(x)cos(2πxt)/60	x	h(x)	(2πxt)/60	cos(2πxt)/60	h(x)cos(2πxt)/6	Hr(t)
0	103	0	1	102.5						6.5006
1	75	0.73267	0.7433934	55.75450769	-1	95	-0.7327	0.7433934	70.62237641	
2	68	1.46533	0.1052676	7.105563076	-2	83	-1.4653	0.1052676	8.684577093	
3	63	2.198	-0.5868829	-36.68018428	-3	73	-2.198	-0.586883	-42.54901377	
4	50	2.93067	-0.9778375	-48.89187322	-4	55	-2.9307	-0.977837	-53.78106054	
5	40	3.66333	-0.866953	-34.67811825	-5	48	-3.6633	-0.866953	-41.18026542	
6	38	4.396	-0.3111368	-11.66763035	-6	40	-4.396	-0.311137	-12.44547238	
7	33	5.12867	0.4043588	13.14166206	-7	30	-5.1287	0.4043588	12.13076498	
8	25	5.86133	0.9123322	22.80830533	-8	25	-5.8613	0.9123322	22.80830533	
9	5	6.594	0.9520847	4.760423624	-9	21	-6.594	0.9520847	19.51773686	
10	1	7.32667	0.5032149	0.503214857	-10	13	-7.3267	0.5032149	6.541793135	
				74.65587054					-9.650258298	

at (t = 8)

x	h(x)	(2πxt)/60	cos(2πxt)/60	h(x)cos(2πxt)/60	x	h(x)	(2πxt)/60	cos(2πxt)/60	h(x)cos(2πxt)/6	Hr(t)
0	103	0	1	102.5						7.2536
1	75	0.83733	0.6694462	50.2084624	-1	95	-0.8373	0.6694462	63.5973857	
2	68	1.67467	-0.1036837	-6.998647293	-2	83	-1.6747	-0.103684	-8.553902247	
3	63	2.512	-0.8082674	-50.5167142	-3	73	-2.512	-0.808267	-58.59938848	
4	50	3.34933	-0.9784994	-48.92496979	-4	55	-3.3493	-0.978499	-53.81746677	
5	40	4.18667	-0.5018379	-20.07351637	-5	48	-4.1867	-0.501838	-23.83730069	
6	38	5.024	0.3065925	11.49721755	-6	40	-5.024	0.3065925	12.26369872	
7	33	5.86133	0.9123322	29.65079693	-7	30	-5.8613	0.9123322	27.3699664	
8	25	6.69867	0.9149221	22.87305338	-8	25	-6.6987	0.9149221	22.87305338	
9	5	7.536	0.31265	1.563250083	-9	21	-7.536	0.31265	6.409325341	
10	1	8.37333	-0.4963174	-0.496317426	-10	13	-8.3733	-0.496317	-6.452126535	
				91.28261525					-18.74675518	

at (t = 9)

x	h(x)	(2πxt)/60	cos(2πxt)/60	h(x)cos(2πxt)/60	x	h(x)	(2πxt)/60	cos(2πxt)/60	h(x)cos(2πxt)/6	Hr(t)
0	103	0	1	102.5						5.1473
1	75	0.942	0.5881717	44.11287977	-1	95	-0.942	0.5881717	55.87631438	
2	68	1.884	-0.308108	-20.79729211	-2	83	-1.884	-0.308108	-25.41891258	
3	63	2.826	-0.9506126	-59.41328738	-3	73	-2.826	-0.950613	-68.91941336	
4	50	3.768	-0.8101389	-40.50694411	-4	55	-3.768	-0.810139	-44.55763852	
5	40	4.71	-0.002389	-0.095559124	-5	48	-4.71	-0.002389	-0.11347646	
6	38	5.652	0.8073286	30.27482338	-6	40	-5.652	0.8073286	32.29314493	
7	33	6.594	0.9520847	30.94275356	-7	30	-6.594	0.9520847	28.56254174	
8	25	7.536	0.31265	7.816250416	-8	25	-7.536	0.31265	7.816250416	
9	5	8.478	-0.5843009	-2.921504611	-9	21	-8.478	-0.584301	-11.97816891	
10	1	9.42	-0.9999886	-0.999988586	-10	13	-9.42	-0.999989	-12.99985161	
				90.9121312					-39.43920996	

at (t =10)

x	h(x)	(2πxt)/60	cos(2πxt)/60	h(x)cos(2πxt)/60	x	h(x)	(2πxt)/60	cos(2πxt)/60	h(x)cos(2πxt)/6	Hr(t)
0	103	0	1	102.5						5.1473
1	75	0.942	0.5881717	44.11287977	-1	95	-0.942	0.5881717	55.87631438	
2	68	1.884	-0.308108	-20.79729211	-2	83	-1.884	-0.308108	-25.41891258	
3	63	2.826	-0.9506126	-59.41328738	-3	73	-2.826	-0.950613	-68.91941336	
4	50	3.768	-0.8101389	-40.50694411	-4	55	-3.768	-0.810139	-44.55763852	
5	40	4.71	-0.002389	-0.095559124	-5	48	-4.71	-0.002389	-0.11347646	
6	38	5.652	0.8073286	30.27482338	-6	40	-5.652	0.8073286	32.29314493	
7	33	6.594	0.9520847	30.94275356	-7	30	-6.594	0.9520847	28.56254174	
8	25	7.536	0.31265	7.816250416	-8	25	-7.536	0.31265	7.816250416	
9	5	8.478	-0.5843009	-2.921504611	-9	21	-8.478	-0.584301	-11.97816891	
10	1	9.42	-0.9999886	-0.999988586	-10	13	-9.42	-0.999989	-12.99985161	
				90.9121312					-39.43920996	

Table (2) : the values of g(x) for standard peak and (x) and Gr(t) at all values of t from 0 to 10,
at(t = 0)

x	g(x)	(2πxt)/60	cos(2πxt)/60	g(x)cos(2πxt)/60	x	g(x)	(2πxt)/60	cos(2πxt)/60	g(x)cos(2πxt)/60	Gr(t)
0	350	0	1	350						310
1	330	0	1	330	-1	320	0	1	320	
2	300	0	1	300	-2	290	0	1	290	
3	200	0	1	200	-3	225	0	1	225	
4	160	0	1	160	-4	150	0	1	150	
5	125	0	1	125	-5	130	0	1	130	
6	105	0	1	105	-6	75	0	1	75	
7	85	0	1	85	-7	45	0	1	45	
8	70	0	1	70	-8	25	0	1	25	
9	50	0	1	50	-9	20	0	1	20	
10	35	0	1	35	-10	10	0	1	10	
				1810					1290	

at (t =1)

x	g(x)	(2πxt)/60	cos(2πxt)/60	g(x)cos(2πxt)/60	x	g(x)	(2πxt)/60	cos(2πxt)/60	g(x)cos(2πxt)/60	Gr(t)
0	350	0	1	350						221.9
1	330	0.2093	0.9781697	322.7959913	-1	320	-0.209	0.97816967	313.0142946	
2	300	0.4187	0.9136318	274.0895427	-2	290	-0.419	0.91363181	264.9532246	
3	200	0.628	0.8092042	161.8408362	-3	225	-0.628	0.80920418	182.0709407	
4	160	0.8373	0.6694462	107.1113864	-4	150	-0.837	0.66944617	100.4169248	
5	125	1.0467	0.5004597	62.55746113	-5	130	-1.047	0.50045969	65.05975957	
6	105	1.256	0.3096228	32.51039537	-6	75	-1.256	0.30962281	23.22171098	
7	85	1.4653	0.1052676	8.947746096	-7	45	-1.465	0.1052676	4.737042051	
8	70	1.6747	-0.103684	-7.257856452	-8	25	-1.675	-0.1036837	-2.59209159	
9	50	1.884	-0.308108	-15.40540156	-9	20	-1.884	-0.308108	-6.162160626	
10	35	2.0933	-0.49908	-17.46780698	-10	10	-2.093	-0.4990802	-4.990801994	
				1279.722294					939.7288432	

at(t = 2)

x	g(x)	(2πxt)/60	cos(2πxt)/60	g(x)cos(2πxt)/60	x	g(x)	(2πxt)/60	cos(2πxt)/60	g(x)cos(2πxt)/60	Gr(t)
0	350	0	1	350						147.17
1	330	0.314	0.9511057	313.8648876	-1	320	-0.314	0.95110572	304.3538304	
2	300	0.628	0.8092042	242.7612543	-2	290	-0.628	0.80920418	234.6692125	
3	200	0.942	0.5881717	117.6343461	-3	225	-0.942	0.58817173	132.3386393	
4	160	1.256	0.3096228	49.53965009	-4	150	-1.256	0.30962281	46.44342196	
5	125	1.57	0.0007963	0.099540839	-5	130	-1.57	0.00079633	0.103522472	
6	105	1.884	-0.308108	-32.35134328	-6	75	-1.884	-0.308108	-23.10810235	
7	85	2.198	-0.586883	-49.88505062	-7	45	-2.198	-0.5868829	-26.40973268	
8	70	2.512	-0.808267	-56.57871991	-8	25	-2.512	-0.8082674	-20.20668568	
9	50	2.826	-0.950613	-47.53062991	-9	20	-2.826	-0.9506126	-19.01225196	
10	35	3.14	-0.999999	-34.99995561	-10	10	-3.14	-0.9999987	-9.999987317	
				852.5539795					619.1718666	

at (t = 3)

x	g(x)	(2πxt)/60	cos(2πxt)/60	g(x)cos(2πxt)/60	x	g(x)	(2πxt)/60	cos(2πxt)/60	g(x)cos(2πxt)/60	Gr(t)
0	350	0	1	350						86.6
1	330	0.4187	0.913632	301.498497	-1	320	-0.419	0.91363181	292.3621789	
2	300	0.8373	0.669446	200.8338496	-2	290	-0.837	0.66944617	194.1393879	
3	200	1.256	0.309623	61.92456261	-3	225	-1.256	0.30962281	69.66513294	
4	160	1.6747	-0.103684	-16.58938618	-4	150	-1.675	-0.1036837	-15.55254954	
5	125	2.0933	-0.49908	-62.38502492	-5	130	-2.093	-0.4990802	-64.88042592	
6	105	2.512	-0.808267	-84.86807986	-6	75	-2.512	-0.8082674	-60.62005705	
7	85	2.9307	-0.977837	-83.11618447	-7	45	-2.931	-0.9778375	-44.00268589	
8	70	3.3493	-0.978499	-68.49495771	-8	25	-3.349	-0.9784994	-24.4624849	
9	50	3.768	-0.810139	-40.50694411	-9	20	-3.768	-0.8101389	-16.20277764	
10	35	4.1867	-0.501838	-17.56432682	-10	10	-4.187	-0.5018379	-5.018379092	
				540.7320051					325.4273398	

at (t = 4)

x	g(x)	(2πxt)/60	cos(2πxt)/60	g(x)cos(2πxt)/60	x	g(x)	(2πxt)/60	cos(2πxt)/60	g(x)cos(2πxt)/60	Gr(t)
0	350	0	1	350						51.51
1	330	0.5233	0.8661581	285.8321712	-1	320	-0.523	0.86615809	277.1705902	
2	300	1.0467	0.5004597	150.1379067	-2	290	-1.047	0.50045969	145.1333098	
3	200	1.57	0.0007963	0.159265342	-3	225	-1.57	0.00079633	0.17917351	
4	160	2.0933	-0.49908	-79.8528319	-4	150	-2.093	-0.4990802	-74.8620299	
5	125	2.6167	-0.865361	-108.1701294	-5	130	-2.617	-0.865361	-112.4969346	
6	105	3.14	-0.999999	-104.9998668	-6	75	-3.14	-0.9999987	-74.99990488	
7	85	3.6633	-0.866953	-73.69100128	-7	45	-3.663	-0.866953	-39.01288303	
8	70	4.1867	-0.501838	-35.12865365	-8	25	-4.187	-0.5018379	-12.54594773	
9	50	4.71	-0.002389	-0.119448906	-9	20	-4.71	-0.002389	-0.047779562	
10	35	5.2333	0.4976994	17.41948053	-10	10	-5.233	0.49769944	4.976994438	
				401.5868917					113.4945882	

at (t = 5)

x	g(x)	(2πxt)/60	cos(2πxt)/60	g(x)cos(2πxt)/60	x	g(x)	(2πxt)/60	cos(2πxt)/60	g(x)cos(2πxt)/60	Gr(t)
0	350	0	1	350						221.9
1	330	0.2093	0.9781697	322.7959913	-1	320	-0.209	0.97816967	313.0142946	
2	300	0.4187	0.9136318	274.0895427	-2	290	-0.419	0.91363181	264.9532246	
3	200	0.628	0.8092042	161.8408362	-3	225	-0.628	0.80920418	182.0709407	
4	160	0.8373	0.6694462	107.1113864	-4	150	-0.837	0.66944617	100.4169248	
5	125	1.0467	0.5004597	62.55746113	-5	130	-1.047	0.50045969	65.05975957	
6	105	1.256	0.3096228	32.51039537	-6	75	-1.256	0.30962281	23.22171098	
7	85	1.4653	0.1052676	8.947746096	-7	45	-1.465	0.1052676	4.737042051	
8	70	1.6747	-0.103684	-7.257856452	-8	25	-1.675	-0.1036837	-2.59209159	
9	50	1.884	-0.308108	-15.40540156	-9	20	-1.884	-0.308108	-6.162160626	
10	35	2.0933	-0.49908	-17.46780698	-10	10	-2.093	-0.4990802	-4.990801994	
				1279.722294					939.7288432	

at(t = 6)

x	g(x)	(2πxt)/60	cos(2πxt)/60	g(x)cos(2πxt)/60	x	g(x)	(2πxt)/60	cos(2πxt)/60	g(x)cos(2πxt)/60	Gr(t)
0	350	0	1	350						36.652
1	330	0.628	0.8092042	267.0373797	-1	320	-0.628	0.80920418	258.9453379	
2	300	1.256	0.3096228	92.88684392	-2	290	-1.256	0.30962281	89.79061579	
3	200	1.884	-0.308108	-61.62160626	-3	225	-1.884	-0.308108	-69.32430704	
4	160	2.512	-0.808267	-129.3227884	-4	150	-2.512	-0.8082674	-121.2401141	
5	125	3.14	-0.999999	-124.9998415	-5	130	-3.14	-0.9999987	-129.9998351	
6	105	3.768	-0.810139	-85.06458262	-6	75	-3.768	-0.8101389	-60.76041616	
7	85	4.396	-0.311137	-26.4466288	-7	45	-4.396	-0.3111368	-14.00115643	
8	70	5.024	0.3065925	21.46147276	-8	25	-5.024	0.30659247	7.664811699	
9	50	5.652	0.8073286	40.36643117	-9	20	-5.652	0.80732862	16.14657247	
10	35	6.28	0.9999949	34.99982244	-10	10	-6.28	0.99999493	9.999949269	
				379.2965025					-12.7785417	

at (t = 7)

x	g(x)	(2πxt)/60	cos(2πxt)/60	g(x)cos(2πxt)/60	x	g(x)	(2πxt)/60	cos(2πxt)/60	g(x)cos(2πxt)/60	Gr(t)
0	350	0	1	350						29.42
1	330	0.7327	0.7433934	245.3198339	-1	320	-0.7327	0.7433934	237.8858995	
2	300	1.4653	0.1052676	31.58028034	-2	290	-1.4653	0.1052676	30.52760433	
3	200	2.198	-0.586883	-117.3765897	-3	225	-2.198	-0.5868829	-132.0486634	
4	160	2.9307	-0.977837	-156.4539943	-4	150	-2.9307	-0.9778375	-146.6756196	
5	125	3.6633	-0.866953	-108.3691195	-5	130	-3.6633	-0.866953	-112.7038843	
6	105	4.396	-0.311137	-32.66936499	-6	75	-4.396	-0.3111368	-23.33526071	
7	85	5.1287	0.4043588	34.37050077	-7	45	-5.1287	0.4043588	18.19614746	
8	70	5.8613	0.9123322	63.86325492	-8	25	-5.8613	0.9123322	22.80830533	
9	50	6.594	0.9520847	47.60423624	-9	20	-6.594	0.9520847	19.0416945	
10	35	7.3267	0.5032149	17.61251998	-10	10	-7.3267	0.5032149	5.032148565	
				375.4815576					-81.2716284	

at (t = 8)

x	g(x)	(2πxt)/60	cos(2πxt)/60	g(x)cos(2πxt)/60	x	g(x)	(2πxt)/60	cos(2πxt)/60	g(x)cos(2πxt)/60	Gr(t)
0	350	0	1	350						20.94
1	330	0.8373	0.6694462	220.9172345	-1	320	-0.8373	0.66944617	214.2227729	
2	300	1.6747	-0.103684	-31.10509908	-2	290	-1.6747	-0.1036837	-30.06826244	
3	200	2.512	-0.808267	-161.6534855	-3	225	-2.512	-0.8082674	-181.8601711	
4	160	3.3493	-0.978499	-156.5599033	-4	150	-3.3493	-0.9784994	-146.7749094	
5	125	4.1867	-0.501838	-62.72973865	-5	130	-4.1867	-0.5018379	-65.2389282	
6	105	5.024	0.3065925	32.19220914	-6	75	-5.024	0.30659247	22.9944351	
7	85	5.8613	0.9123322	77.54823812	-7	45	-5.8613	0.91233221	41.05494959	
8	70	6.6987	0.9149221	64.04454946	-8	25	-6.6987	0.91492214	22.87305338	
9	50	7.536	0.31265	15.63250083	-9	20	-7.536	0.31265002	6.253000333	
10	35	8.3733	-0.496317	-17.3711099	-10	10	-8.3733	-0.4963174	-4.963174257	
				330.9153957					-121.5072341	

at (t = 9)

x	g(x)	(2πxt)/60	cos(2πxt)/60	g(x)cos(2πxt)/60	x	g(x)	(2πxt)/60	cos(2πxt)/60	g(x)cos(2πxt)/60	Gr(t)
0	350	0	1	350						10.77
1	330	0.942	0.5881717	194.096671	-1	320	-0.942	0.58817173	188.2149537	
2	300	1.884	-0.308108	-92.43240938	-2	290	-1.884	-0.308108	-89.35132907	
3	200	2.826	-0.950613	-190.1225196	-3	225	-2.826	-0.9506126	-213.8878346	
4	160	3.768	-0.810139	-129.6222211	-4	150	-3.768	-0.8101389	-121.5208323	
5	125	4.71	-0.002389	-0.298622264	-5	130	-4.71	-0.002389	-0.310567155	
6	105	5.652	0.8073286	84.76950545	-6	75	-5.652	0.80732862	60.54964675	
7	85	6.594	0.9520847	80.92720161	-7	45	-6.594	0.95208472	42.84381262	
8	70	7.536	0.31265	21.88550117	-8	25	-7.536	0.31265002	7.816250416	
9	50	8.478	-0.584301	-29.21504611	-9	20	-8.478	-0.5843009	-11.68601844	
10	35	9.42	-0.999989	-34.99960049	-10	10	-9.42	-0.9999886	-9.999885856	
				254.9884602					-147.3318039	

at (t =10)

x	g(x)	(2πxt)/60	cos(2πxt)/60	g(x)cos(2πxt)/60	x	g(x)	(2πxt)/60	cos(2πxt)/60	g(x)cos(2πxt)/60	Gr(t)
0	350	0	1	350						3.2747
1	330	1.0467	0.5004597	165.1516974	-1	320	-1.047	0.50045969	160.1471005	
2	300	2.0933	-0.49908	-149.7240598	-2	290	-2.093	-0.4990802	-144.7332578	
3	200	3.14	-0.999999	-199.9997463	-3	225	-3.14	-0.9999987	-224.9997146	
4	160	4.1867	-0.501838	-80.29406548	-4	150	-4.187	-0.5018379	-75.27568638	
5	125	5.2333	0.4976994	62.21243047	-5	130	-5.233	0.49769944	64.70092769	
6	105	6.28	0.9999949	104.9994673	-6	75	-6.28	0.99999493	74.99961952	
7	85	7.3267	0.5032149	42.7732628	-7	45	-7.327	0.50321486	22.64466854	
8	70	8.3733	-0.496317	-34.7422198	-8	25	-8.373	-0.4963174	-12.40793564	
9	50	9.42	-0.999989	-49.99942928	-9	20	-9.42	-0.9999886	-19.99977171	
10	35	10.467	-0.504591	-17.66066846	-10	10	-10.47	-0.5045905	-5.045905274	
				192.7166688					-159.9699552	

Table (3): The values of F(L), H(L) and G(L) for different values of (t) of the line (111) .

T	Hr(t)	Gr(t)	Fr(t)
0	97.95	310	0.315967742
1	88.30670982	285	0.309848105
2	63.97051823	221.9451137	0.288226747
3	35.83393255	147.1725846	0.243482389
4	14.51123008	86.61593449	0.167535341
5	4.69313383	51.508148	0.091114397
6	4.023019793	36.65179608	0.109763237
7	6.500561224	29.42099292	0.220949757
8	7.253586007	20.94081616	0.346385067
9	5.147292124	10.76566563	0.478121121
10	2.014269707	3.274671358	0.61510591
			0.318649981

Table (4) : The values of F(L), H(L) and G(L) for different values of (t) of the line (200).

T	Hr(t)	Gr(t)	Fr(t)
0	194.8	310	0.628387097
1	178.5383399	285	0.626450315
2	136.4207732	221.9451137	0.614659953
3	84.7213454	147.1725846	0.575659833
4	40.5891308	86.61593449	0.468610436
5	13.88546928	51.508148	0.269578112
6	4.317448632	36.65179608	0.117796373
7	4.648396928	29.42099292	0.157995923
8	6.800855001	20.94081616	0.324765518
9	6.47191163	10.76566563	0.601162237
10	3.865128068	3.274671358	1.180310219
			0.556537601

Table (5) : The values of F(L), H(L) and G(L) for different values of (t) of the line (220).

T	Hr(t)	Gr(t)	Fr(t)
0	105.25	310	0.339516129
1	97.16058778	285	0.340914343
2	76.16266043	221.9451137	0.343159888
3	50.21820305	147.1725846	0.341219822
4	27.67395791	86.61593449	0.319501926
5	13.2936714	51.508148	0.258088709
6	6.952381569	36.65179608	0.189687336
7	5.292067696	29.42099292	0.179873865
8	4.677980134	20.94081616	0.223390535
9	3.300237873	10.76566563	0.306552143
10	1.359523446	3.274671358	0.415163324
			0.325706802

Table (6): The values of F(L), H(L) and G(L) for different values of (t) 0f the line (311).

T	Hr(t)	Gr(t)	Fr(t)
0	39.725	310	0.12814516
1	36.49194207	285	0.1280419
2	28.14239672	221.9451137	0.1267989
3	17.94608403	147.1725846	0.12193904
4	9.284208234	86.61593449	0.10718822
5	4.003429094	51.508148	0.07772419
6	1.916796361	36.65179608	0.05229747
7	1.561466367	29.42099292	0.0530732
8	1.475775317	20.94081616	0.07047363
9	1.051519526	10.76566563	0.09767343
10	0.514665625	3.274671358	0.15716558
			0.11205207

Table (7) : The values of F(L), H(L) and G(L) for different values of (t)of the line (222).

T	Hr(t)	Gr(t)	Fr(t)
0	0.903	310	0.002912903
1	27.8958703	285	0.097880247
2	20.7559573	221.9451137	0.093518424
3	12.1608306	147.1725846	0.082629728
4	5.12112151	86.61593449	0.059124473
5	1.27092149	51.508148	0.024674183
6	0.38225188	36.65179608	0.010429281
7	1.00718977	29.42099292	0.034233711
8	1.63675286	20.94081616	0.078160892
9	1.54896944	10.76566563	0.143880508
10	0.90375871	3.274671358	0.275984551
			0.09034289

Table (8) : the crystallite size and lattice strain for the lines (111), (200) ,(220) , (311) and (222) of the x- ray diffraction of MnO nanoparticle for Fourier method .

Peak (hkl)	2θ degree	θ degree	d nm	L nm	D nm	$< \varepsilon^2 > \times 10^{-4}$
111	35.5	17.75	0.2527	6.162	5.3885	0.9699
200	40.6	20.3	0.222	9.427	16.087	0.1648
220	59	29.5	0.1564	10.162	9.0594	0.134
311	74.25	37.125	0.1276	8.854	3.6828	0.2583
222	70.75	35.375	0.133	8.753	3.9999	0.2562
					7.64352	0.35664

Table (9) : The particle size and strain calculation for the lines (111) , (200) , (220) , (311) and (222) for Debye – Scherrer method .

Peak	β(2θ)redian	θ degree	4tan(θ)	cos(θ)	D nm	ε×10^-4
111	0.02128	17.75	1.2804	0.95239	6.7647	166.2126
200	0.01788	20.3	1.47964	0.93788	8.1731	120.8398
220	0.01293	29.5	2.26308	0.87142	8.7094	79.930608
311	0.02289	35.375	2.84002	0.81538	7.3445	80.6182
222	0.02253	37.125	3.02792	0.75698	7.6324	74.0752
					7.72482	104.33528

Table (10): The values of FWHM $\cos\theta$ and $4\sin\theta$ for the lines (111) , (200) , (220) , (311) and (222) by Williamson –Hall method of XRD pattern of MnO nanoparticles .

Peak	FWHM radian	θ degree	COS(θ)	FWCOS(θ)	SIN(θ)	4SIN(θ)
111	0.021282	17.75	0.952395	0.0202688	0.304864	1.219456
200	0.0178805	20.3	0.937888	0.016769	0.3469356	1.3877424
220	0.018089	29.5	0.870355	0.0157438	0.4924235	1.969694
311	0.0228958	35.375	0.81538	0.018668	0.578925	2.3157
222	0.0179644	37.125	0.79732	0.017964	0.603555	2.41422

Table (11) : The values of $\ln(1 / \cos\theta)$ and values $\ln\beta$ of the lines (111) , (200) , (220) , (311) and (222) for the Modified Scherrer method .

Peak (hkl)	θ	θ redian	COS(θ)	1/cos(θ)	ln1/cos(θ)	$\beta(2\theta)$ redian	$\ln\beta(2\theta)$
111	17.75	0.309639	0.952444	1.049931	0.048724	0.02027	-3.8986
200	20.3	0.354122	0.937951	1.066154	0.064057	0.01678	-4.0878
220	29.5	0.514611	0.870484	1.148786	0.138706	0.01574	-4.1513
311	35.375	0.617097	0.815562	1.226149	0.203878	0.01867	-3.9809
222	37.125	0.647625	0.797519	1.253889	0.22625	0.01796	-4.0193

Table (12): The results of crystallite size and lattice strain of the Fourier analysis method , Debye – Sherrer method , Williamson-hall method , Modified Scherrer method.

Forier Analysis Method		Deby-scherrer Method		Modifical Scherrer Method	Williamsos -hall Method	
D nm	<ε^2>*10^-4	D nm	ε*10^-4	D nm	D nm	ε*10^-4
7.6435	0.3566	8.4167	99.8351	6.508	9.8642	20.833

Refrence

T. Ungar and J. Gubicza .Department of General Physics, Eotvos University Budapest, H-1518, P.O.B 32,

Budapest,Hungary .
Hongqiang Chen, Y. Lawrence Yao, Jeffrey Kysar, Youneng Wang .Department of Mechanical Engineering .Columbia University, New York, NY 10027. Transactions of NAMRI/SME , Volume 32, 2004.
K KAPOOR*, D LAHIRI, S V R RAO, T SANYAL and B P KASHYAP† .Bull. Mater. Sci., Vol. 27, No. 1, February 2004, pp. 59–67. © Indian Academy of Sciences.
ROBERT M. STROUD AND DAVID A. AGARD, Department o Biochemistry and Biophysics, University ofCalifornia, San Francisco, California 94143 U.S.A. BIoPHYsJ. @Biophysical Society * 0006-3495/79/03/495/18 495, Volume 25 March 1979 495-512
D. Balzar ,a ,b* N. Audebr and ,c M. R. Daymond ,d A. Fitch ,e A. Hewat ,f J. I.Langford ,g A. Le Bail ,h D. Loue¨r ,c O. Masson ,e C. N. McCowan ,b N. C. Popa,I P. W. Stephensj and B. H. Tobyk.J. Appl. Cryst. (2004). 37, 911–924.
Berman, R.M. and I. Cohen, Method for improve x-ray diffraction determinations of residual stress in nickel-base alloys. 1990.
Liquid-Mix Disorder in Crystalline Solids: ScMnO .P. Karen & P.M. Woodward, J. Solid State Chem. 141, 78-88 (1998) .
B. E. Warren ,X-Ray Diffaction ,Addison –Wesley Publishing Company ,1969.
A. R. Stokes, Proc. Soc .London 61(1948) 382.
S. Vives , E.Gaffet , CMeunier , Materials Science and Engineering A366 (2004)229-238,
L. P. Smith, Phys. Rev. 46, 343 (1934).
A. R. Stokes, Proc. Phys. Soc. Lond. 61, 382 (1948).
H. C. Burger and P. H. van Cittert, Z. Phys. 79, 722 (1932).
S. Ergun, J. Appl. Ciyst. 1, 19 (1968).
H.P.Klug, L.Alexander , X-Ray Diffraction Polycrystalline and Amorphous Materials ,2^{nd}ed.John Wiley and Sons , New York 1974.
F. Raiteri, A. Senin, G. Fagherazzi ,J Mater. Science 13, 1717(1978).
D. Taupin, J. Appl. Cryst. 6, 266 (1973).
T. C. Huang and W. Parrish, Appl. Phys. Lett. 27, 123.
A.Patterson, The scherrer formula for X-Ray P article size deter mination ,phys.Rev.56(10)(1939)978-982.
P. scherrer, Gottinger Nachrichten .Gesell 2(1918)(98-100) .
S. N . Anitha, l. Jayakumar ,Journal of Nanoscience and Technology (1)(2015)26-31.
Eric J. Mittemeijer* and Udo Welzel ,Max Planck Institute for Metals Research, Heisenbergstraße 3, 70569 Stuttgart, Germany , Z. Kristallogr. 223 (2008) 552–560 / DOI 10.1524/zkri.2008.1213 .
Delhez, R.; de Kejser, Th. H.; Mittemeijer, E. J.: Determination of crystallite size and lattice distortions through X-ray diffraction line profile analysis. Fresenius Z. Anal. Chem. 312 (1982) 1–16 .
24- http://pd.chem.ucl.ac.uk/pdnn/peaks/size.htm.
A. R. Stokes, A. J. C. Wilson, Proc. Phys. Soc. (London, U. K.) 56 (1944) 174–181.
D. Balzar, N. Audebrand, M. R. Daymond, A. Fitch, A.Hewat, J. I. Langford, A. Le Bail, D. Louër, O. Masson, C.N. McCowan, N. C. Popa, P. W. Stephens, B. H. Toby, J.Appl. Crystallogr. 37 (2004) 911–924.
G. K. Williamson, W. H. Hall, Acta Metall. 1 (1953) 22–31.
W. H. Hall, Proc. Phys. Soc. A (London, U. K.) 62 (1949) 741–743.
E. H. Kisi, C. J. Howard, "Applications of Neutron Powder Diffraction," Oxford University Press, New York.
FujioIzumi*,**, Takuji Ikeda***,先進セラミックス研究センター年報 （2014） . Vol. 3, 33-38 .